Dalton Transactions

PAPER

View Article Online
View Journal

Cite this: DOI: 10.1039/c4dt02981j

Towards understanding the design of dual-modal MR/fluorescent probes to sense zinc ions†

Charlotte Rivas,[a] Graeme J. Stasiuk,[a,b] Myra Sae-Heng[a] and Nicholas J. Long*[a]

Received 26th September 2014,
Accepted 18th December 2014

DOI: 10.1039/c4dt02981j

www.rsc.org/dalton

A series of gadolinium complexes were synthesised in order to test the design of dual-modal probes that display a change in fluorescence or relaxivity response upon binding of zinc. A dansyl-DO3ATA gadolinium complex **[GdL^1]** displayed an increase and a slight blue-shift in fluorescence in the presence of zinc; however, a decrease in relaxation rate was observed. Consequently, the ability of the well-known zinc chelator, **BPEN**, was assessed for relaxivity response when conjugated to the gadolinium chelate. The success of this probe **[GdL^2]**, lead to the inclusion of the same zinc-probing moiety alongside a longer wavelength emitting fluorophore, rhodamine **[GdL^3]**, to arrive at the final iteration of these first generation dual-modal zinc-sensing probes. The compounds give insight into the design protocols required for the successful imaging of zinc ions.

Introduction

Being the second most abundant transition metal ion in the body, Zn^{2+} plays a vital role in a vast variety of biological processes.[1] Properties such as its Lewis acidic nature are critical to its enzymatic activity,[2] and its lack of ligand field stabilization energy (LFSE) conferring flexibility in its coordination geometry allowing for a variety of structural motifs,[3] joined together with its kinetic lability of coordinated ligands means that Zn^{2+} plays a major role within proteins. The majority of biological Zn^{2+} is bound within these protein structures and zinc pools exist in certain tissues to maintain homeostasis. The disruption of this homeostasis has been linked with a number of diseases but is poorly understood and as such, it is becoming increasingly important to develop probes that can detect Zn^{2+} in biological systems.

Due to its d^{10} electron configuration, Zn^{2+} is a difficult ion to detect, as it is spectroscopically silent. Therefore sensor molecules must be designed so that Zn^{2+} binding induces a characteristic change in the molecule, which can then be signalled *via* an imaging modality. Magnetic resonance (MR) and optical imaging are two modalities that lend themselves well to this sensing field, and their combination offers synergistic advantages. Optical imaging probes boast high sensitivity,[4] an attribute that is lacking in MRI, whilst MRI has high special resolution and good soft-tissue contrast.[5] As such the combination of the two leads to the potentially powerful approach for the quantitative integration of molecular and cellular information within an intact and complex body, as opposed to the isolated *in vitro* systems.[6] Optical imaging alone has produced a vast number of zinc fluorescent chemosensors, many of which have been reviewed extensively[7] and a number of dual-modal MR/optical imaging agents based on Gd^{3+} have been reported in the literature.[8] However, few 'smart' dual-modal probes have been designed that respond to metal ions in a biological setting. Luo *et al.* conjugated the fluorescent Zn^{2+} sensor 8-sulfonamidoquinoline to a Gd-DO3A moiety to produce a probe that displayed a 55% enhancement in r_1 (3.8 to 5.9 mM^{-1} s^{-1}) and a 7-fold increase in fluorescence in the presence of 0.5 equivalents on Zn^{2+}.[9] These findings are the result of the formation of a 1 : 2 binding stoichiometry between GdL and Zn^{2+} at 0.5 eq. At a 1 : 1 stoichiometry, the dianionic 8-sulfonamidoquinoline unit acts as a terdentate ligand resulting in a red-shift to 520 nm due to increased π conjugation and a slight lowering of the relaxivity value to 5.2 mM^{-1} s^{-1} was observed. The overall increase in relaxivity was attributed to the increased molecular weight for the Zn^{2+} complexes and improved molecular rigidity.

In order to arrive at responsive dual-modal MR/optical probes that exhibit changes in both fluorescence and relaxivity a number of properties should be considered. A change in the number of inner-sphere water molecules (q), the rotational tumbling time (τ_R) and the residence lifetime of inner-sphere water molecules (τ_m) will induce a change in relaxivity according to the Solomon–Bloembergen–Morgan equation.[10] The probe must also display good selectivity for Zn^{2+} over other

[a]*Department of Chemistry, Imperial College London, South Kensington Campus, London, SW7 2AZ, UK. E-mail: n.long@imperial.ac.uk*
[b]*School of Biological, Biomedical and Environmental Sciences, University of Hull, Cottingham Road, Hull, HU6 7RX, UK*

†Electronic supplementary information (ESI) available: Details of synthesis and spectroscopic characterisation of all the compounds, metal binding titrations and relaxation measurements. See DOI: 10.1039/c4dt02981j

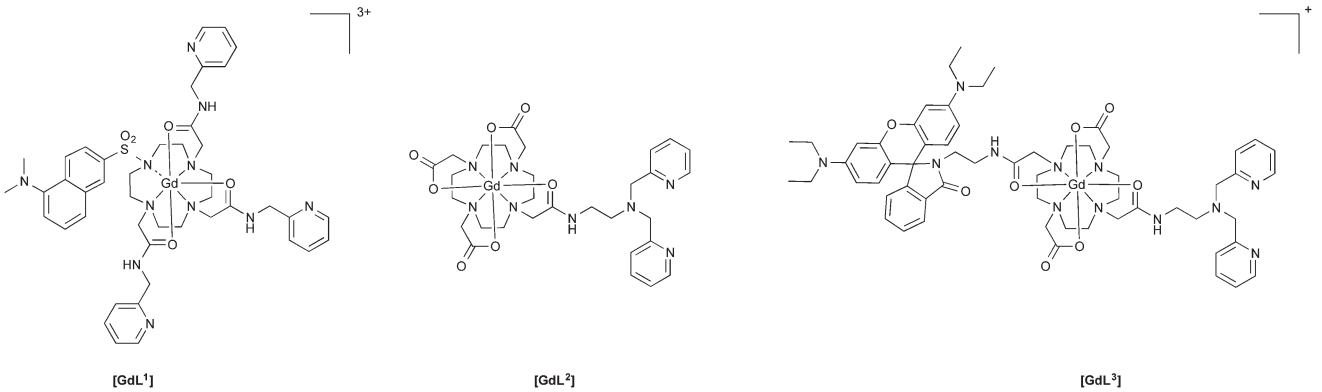

Fig. 1 Structures of the [GdL^{1-3}] complexes reported herein.

biologically relevant cations such as Ca^{2+}, Mg^{2+} and K^{+} and be stable and soluble in biological media. Picolylamine and dipicolylamine (dpa) units have been used as the most popular binding moieties to construct Zn^{2+} sensors.[11] The dpa unit has been used extensively as part of a fluorescent construct but its use as part of an MR active probe has been less studied. Nagano *et al.* first prepared a Gd^{3+} complex using the diethylenetriaminepentaacetic acid (DTPA) ligand bifunctionalised with *N*,*N*-bis-(2-pyridyl-methyl) ethylene diamine (**BPEN**), a derivative of dpa.[12] In the presence of 1 equivalent of Zn^{2+} the relaxivity of the complex decreased from an initial value of 6.1 to 4.0 mM^{-1} s^{-1}. The initial value was obtained upon addition of a further equivalent of Zn^{2+}. Due to the increased thermodynamic stability and kinetic inertness of DOTA-like macrocyclic ligands compared to DTPA, Esqueda *et al.* prepared a GdDOTA-bisBPEN diamide complex.[13] In the presence of 1 equivalent of Zn^{2+} the relaxivity increased from 5 to 6 mM^{-1} s^{-1}. The 1 : 2 GdL : Zn^{2+} was found to bind strongly to human serum albumin (HSA) resulting in a 165% increase in relaxivity to 17.4 mM^{-1} s^{-1}. This significant increase was attributed to a slower τ_R for the complex when bound to the protein.

In an attempt towards the formation of Gd^{3+}-based responsive agents with potential application as dual-modal MR/optical probes, herein we report three classes of heteroditopic ligands [GdL^{1-3}] (Fig. 1), which vary in fluorophore and Zn^{2+} binding unit.

Results and discussion

[GdL^1]

Naphthalene-based fluorophores such as dansyl chloride have been used extensively in fluorescence imaging, and their core-structure can be found in the structure of many fluorescent probes used for the detection of metal ions as well as labels for amino acids, peptides and proteins.[14] It displays spectral properties such as strong fluorescence emission and large Stokes shift, as well as being sensitive to perturbations in local environment, and examples can be found of its conjugation to DOTA-monoamide derivatives to give pH sensors or to investigate energy transfer mechanisms between it and lanthanide ions.[15] As such it was selected as the fluorescent moiety in the first iteration of our dual-modal MR/optical zinc sensing probes.[16]

The dansyl-DO3A-trisamide (DO3ATA) conjugate $\mathbf{L^1}$ was synthesised *via* two routes, both of which involved a four-step synthesis. The first route involved the reaction of amino pyridine with chloroacetyl chloride to form the amide methyl chloride **1**. Reaction of **1** with cyclen under basic conditions yielded the DO3ATA derivative **3**. Conjugation of dansyl chloride to the remaining secondary nitrogen on cyclen gave $\mathbf{L^1}$ (Scheme 1). The preferred route, however, was to first conjugate the dansyl chloride to the cyclen core giving **2**, and then tri-substitution with the amide methyl chloride derivative **1** gave $\mathbf{L^1}$ (dashed box, Scheme 1). This second route was preferred simply due to the dansyl moiety allowing for a fluorescence handle during purification using column chromatography. The dansyl-DO3ATA conjugate $\mathbf{L^1}$ was then complexed with gadolinium to give [$\mathbf{GdL^1}$] in 84% yield.

The fluorescence properties of [$\mathbf{GdL^1}$] were studied and it was found that excitation at 260 nm induced fluorescence emission at 500 nm, as expected for a dansyl derivative. Upon addition of zinc a slight fluorescence response was observed (Fig. 2a). Upon zinc chelation there was a small shift in emission wavelength of 10 nm from 500 to 490 nm and a 5% increase in intensity. This fluorescence response was found to be unique for zinc; when binding studies with other biologically relevant cations such as calcium and copper were carried out, no change in fluorescence was observed (ESI Fig. S2†). The dissociation constants were determined as 44.1 μM (Zn^{2+}), 364 μM (Ca^{2+}), 19 μM (Cu^{2+}) and 5.59 mM (Mg^{2+}), suggesting that [$\mathbf{GdL^1}$] binds preferentially in the order Cu > Zn > Ca > Mg. The low affinities for Mg^{2+} and Ca^{2+} can be attributed to the coordination geometry and size not being ideal for these group two cations. The high affinity for Cu^{2+} is hypothesised to be due to the octahedral geometry being more favourable than the tetrahedral shape of Zn^{2+} as the metal centres are of a similar size and charge. It must be noted that this compound is susceptible to transmetallation with Zn^{2+}. This has been observed in the fluorescence spectrum, as when an excess of

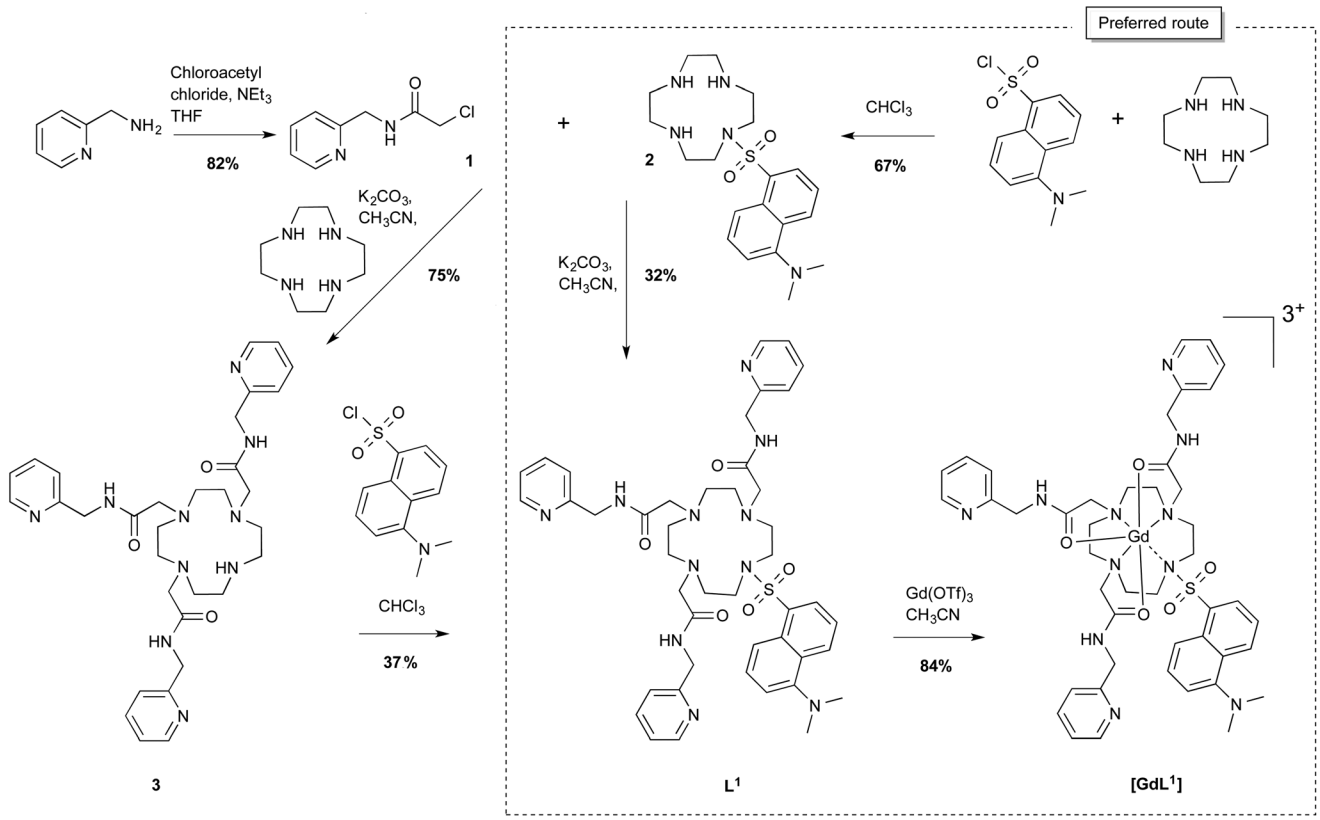

Scheme 1 Scheme of the synthesis of the dansyl-DO3AMA complex **[GdL^1]**.

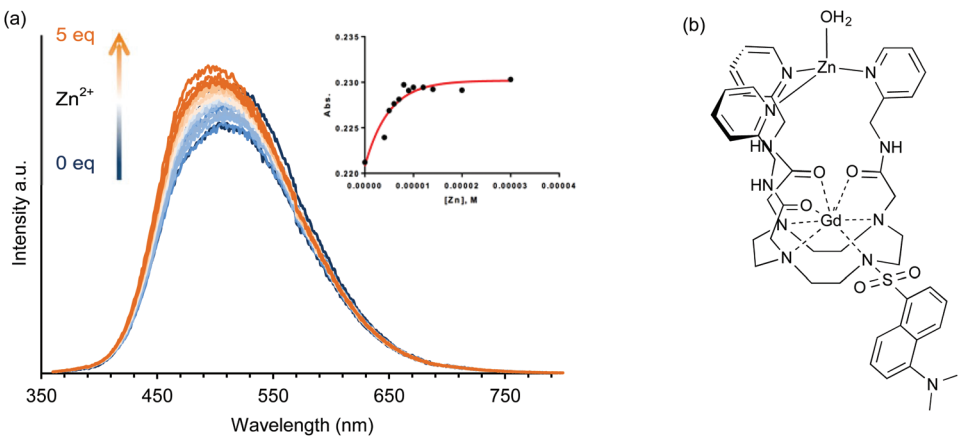

Fig. 2 (a) Fluorescence spectrum of **[GdL^1]** (100 μM) in MeOH in the presence of increasing concentrations (0 to 5 eq.) (λ_{ex} = 335 nm) of Zn^{2+}; (b) proposed steric hindrance around the gadolinium centre induced by coordination of zinc to **[GdL^1]**.

10 equivalents of Zn^{2+} is added there is a significantly large increase in emission intensity which mirrors coordination to the cyclen motif observed by Koike *et al.*[15] This is due to the unstable nature of the amide carbonyl bound Gd^{3+}.

Relaxation measurements of **[GdL^1]** (400 MHz (9.4 T)) show an r_1 = 3.8 mM^{-1} s^{-1}, which suggests a hydration state (q) of one much like the 'gold standard' MRI contrast agent Gd·DOTA (r_1 = 4.2 mM^{-1} s^{-1}).[17] This is unexpected as the co-ordinating ligands suggest that two water ligands should bind (q = 3).[18] It is hypothesised that the dansyl and pyridyl arms must provide a large steric hindrance to block extra water ligands from binding to the Gd(III) metal centre. Also, the three amide coordinating arms are thought to slow water exchange rates. Lower than expected relaxation rates have also been observed by Mishra *et al.* with a FITC moiety conjugated to a DO3A motif with an r_1 of 5.36 mM^{-1} s^{-1}.[19] The relaxation rate (r_1) of **[GdL^1]** is not significantly changed when binding to zinc. In the presence of 1 equivalent of Zn^{2+} the relaxivity

decreases from 3.8 to 3.2 mM^{-1} s^{-1}. It is postulated that the binding of Zn(II) ions further restricts access of the water molecules to the Gd(III) metal centre (Fig. 2b).

[GdL^1] is a good starting point for zinc sensing dual-modal contrast agents. It has an emission at 500 nm and binds Zn with a high affinity over other endogenous anions, but it does fall short in that the relaxation rate decreases. It must be noted that the compound is not 100% soluble in water and requires 10% methanol to be dissolved, and so along with the stability issue and the non-NIR fluorescence it is not ideal for *in vivo* studies. Thus, it was decided to further design the probes to be NIR active and with a higher binding affinity for Zn(II).

[GdL^2]

It is well known that *N*,*N*-bis-(2-pyridyl-methyl)ethylene diamine (**BPEN**) has a high selectivity for Zn^{2+} ions over other biologically relevant metal ions such as Ca^{2+} or Mg^{2+}.[20] This zinc binding moiety has been used by Nagano *et al.* to develop a probe that displays a K_d for Zn^{2+} of 59 nM, a value which allowed its application within biological systems.[21] For this reason, **[GdL^2]** was developed as a zinc binding MR probe. **BPEN** was prepared using a previously reported procedure following protection–derivatisation–deprotection schemes.[21] **BPEN** was then treated with chloroacetyl chloride to obtain compound **4** which was then suitable for conjugation to DO3A under basic conditions (Scheme 2). Removal of the *tert*-butyl groups with trifluoroacetic acid (TFA) yielded **L^2**. The ligand was coordinated to Gd^{3+} in a mildly acidic aqueous environment (pH ~ 5.5) (Scheme 2). After purification using a Sephadex G-10 ion desalting resin, the absence of free lanthanide ions was verified by using xylenol orange indicator solution.[22]

T_1 measurements of **[GdL^2]** were performed at 400 MHz (9.4 T, 25 °C), and their r_1 values over a range of Zn^{2+} concentrations were determined. The relaxivity of **[GdL^2]** increased with addition of Zn^{2+}. In the absence of Zn^{2+}, the relaxivity of the complex was 4.97 mM^{-1} s^{-1} (0.1 M HEPES buffer). This value increased approximately 10% with addition of Zn^{2+} until it levelled at 5.39 mM^{-1} s^{-1} at equivalents of 1 and above. This small yet significant change in relaxivity is thought to be a consequence of the binding of Zn^{2+} creating a more organised second sphere of water molecules (those bound to Zn^{2+}).

UV-vis spectroscopy can also be used to study the binding of Zn^{2+} to the **BPEN** unit; the pyridine groups give a characteristic absorption at λ_{max} = 261 nm which can be monitored over the addition of metal ions.[23] The absorbance between 230 and 300 nm changed linearly with increasing concentrations of Zn^{2+} up to a 1 : 1 Zn^{2+}-**[GdL^2]** molar ratio, with isosbestic points at 252, 264 and 269 nm and remained at a plateau with further increase of Zn^{2+} (Fig. 3, left). These significant variations in the absorption spectrum upon addition of Zn^{2+} indicate that metal-binding is indeed occurring and as such the binding constant was determined to be 55.7 μM. The effect of adding Mg^{2+}, Ca^{2+} and Cu^{2+} on the absorption profile was also examined. The addition of Ca^{2+} and Mg^{2+} showed a negligible effect on the absorption spectra of **[GdL^2]** (246 μM and unfittable, respectively) whilst the addition of Cu^{2+} provoked a significant increase and shift of the absorption maxima toward shorter wavelengths (*ca.* 256 nm) (Fig. 3, right). Although a greater change in absorption was observed with Cu^{2+} compared to Zn^{2+}, a comparison of binding constants (13.8 mM *vs.*

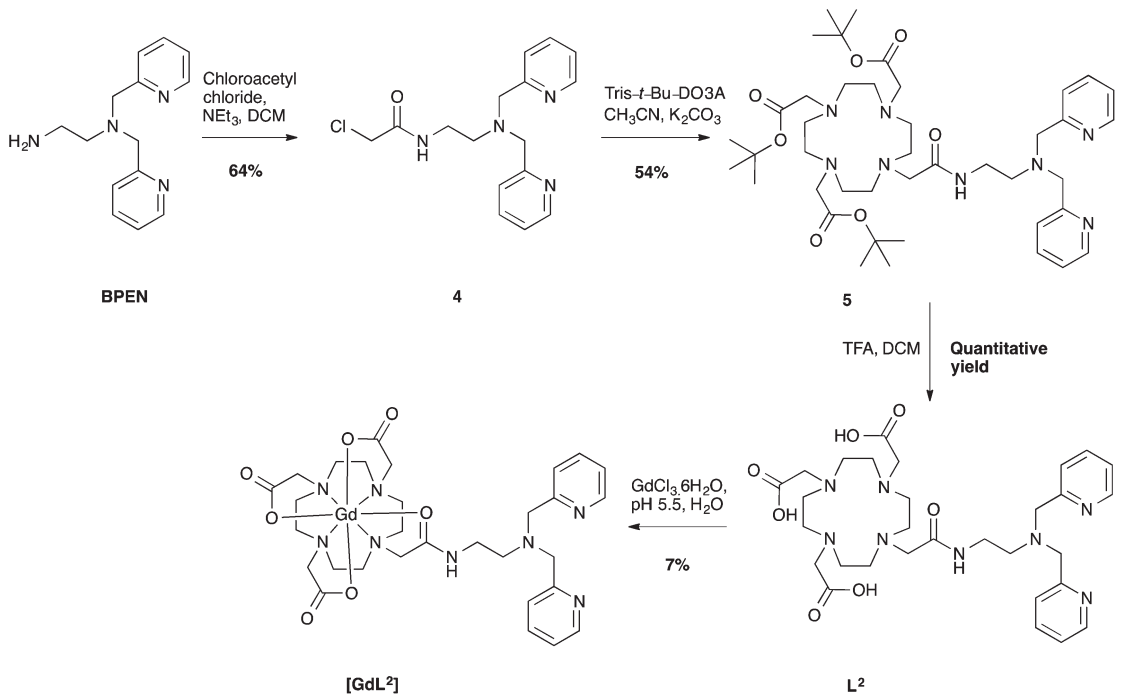

Scheme 2 Synthesis of **BPEN**-DO3A conjugate **GdL^2**.

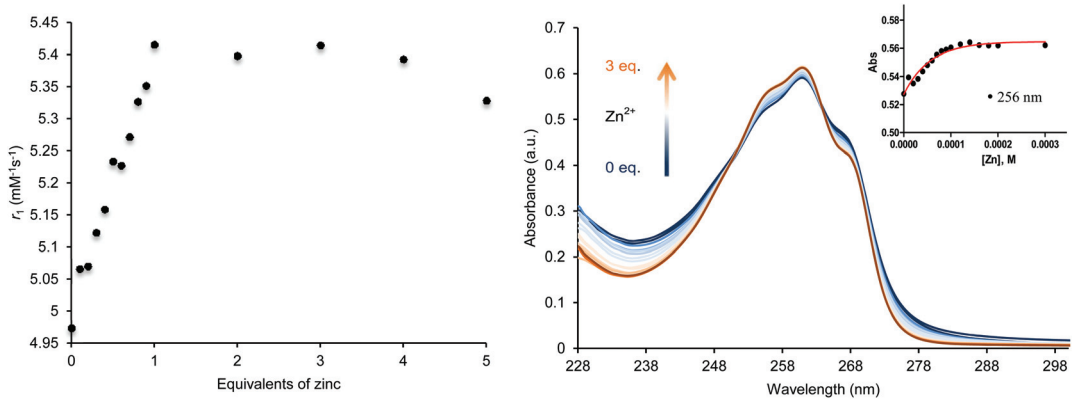

Fig. 3 (Left) Water proton relaxivity of **GdL^2** (pH 7.4, 5 mM) in the presence of increasing concentrations (0 to 5 eq.) of Zn^{2+}; (right) UV/vis spectra of **GdL^2** (100 μM) in HEPES buffer (0.1 M; pH = 7.4) in the presence of increasing concentrations (0 to 3 eq.) of Zn^{2+}.

55.7 μM) indicates a clear preferential binding for Zn^{2+} over other biological metal ions showing that the **BPEN** fragment is suitable as a Zn^{2+}-specific chelator.

[GdL^3]

As it was found that complex **[GdL^2]** functioned successfully as an MR active zinc-sensing probe, it was next decided to further modify the molecule to include a fluorescent moiety that would allow dual-modal imaging. It was also decided to improve on the fluorescence properties that we observed for **[GdL^1]** in order to have a probe which displayed improved tissue penetration through the use of longer emission wavelengths. Rhodamine derivatives have received significant attention as fluorescent chromophores due to their attractive fluorescence properties such as long absorption and emission wavelengths, large absorption coefficients and high quantum yields.[24] The non-trivial synthesis of **L^3** commenced with the conjugation of the rhodamine derivative **5** (synthesis described by Rivas *et al.*[8]) onto ^{t}Bu-DO2A resulted in the tri-substituted compound **6.** Subsequent substitution of the final secondary amine on cyclen with **BPEN 4** produced the pro-ligand **7**. Removal of the *tert*-butyl groups with trifluoroacetic acid (TFA) yielded **L^3**. The ligand was coordinated to Gd^{3+} in a mildly acidic aqueous environment (pH ~ 5.5) resulting in the formation of the dual-modal MR/fluorescent probe **[GdL^3]** (Scheme 3).

The resulting gadolinium complex proved to be water insoluble and as such, fluorescence titrations and relaxivity experiments were carried out in a 50 : 50 MeOH–water (HEPES) solvent mixture. T_1 measurements of **[GdL^3]** were performed at 400 MHz (9.4 T, 25 °C), and their r_1 values over a range of Zn^{2+} concentrations were determined. The observed relaxation rate was 2.94 mM^{-1} s^{-1} and upon zinc binding increased to 3.88 mM^{-1} s^{-1}. This lower than expected relaxation rate could

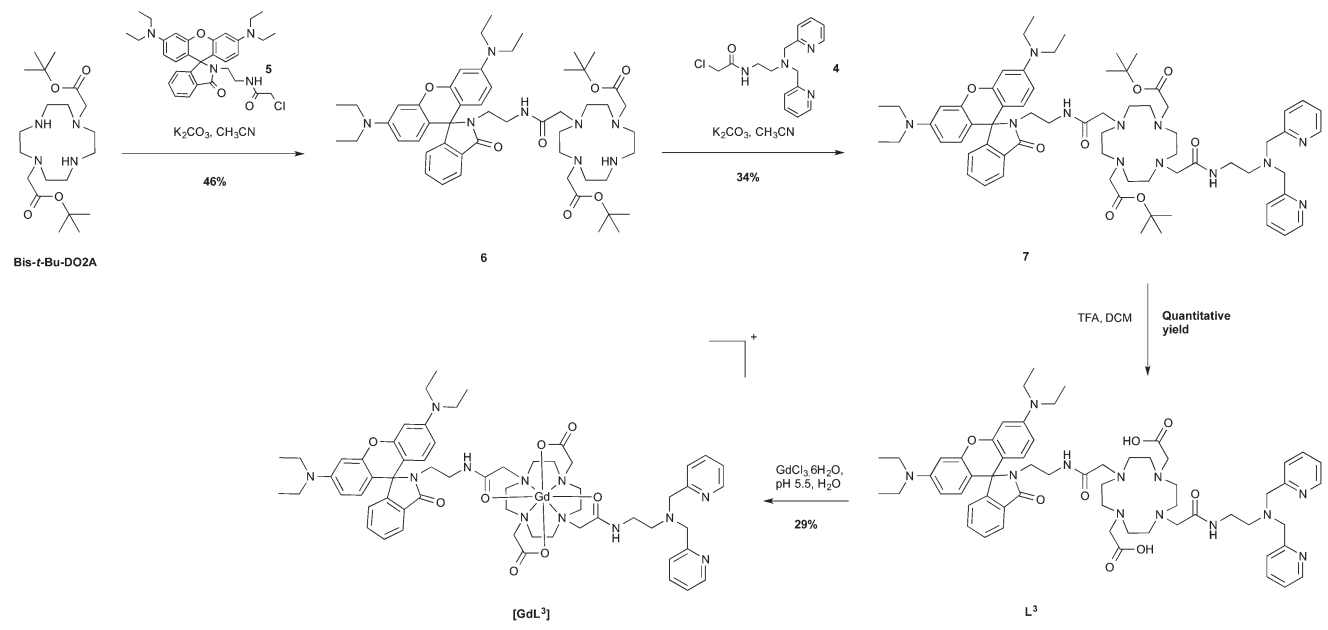

Scheme 3 Synthesis of the rhodamine-**BPEN**-DO2A conjugate **[GdL^3]**.

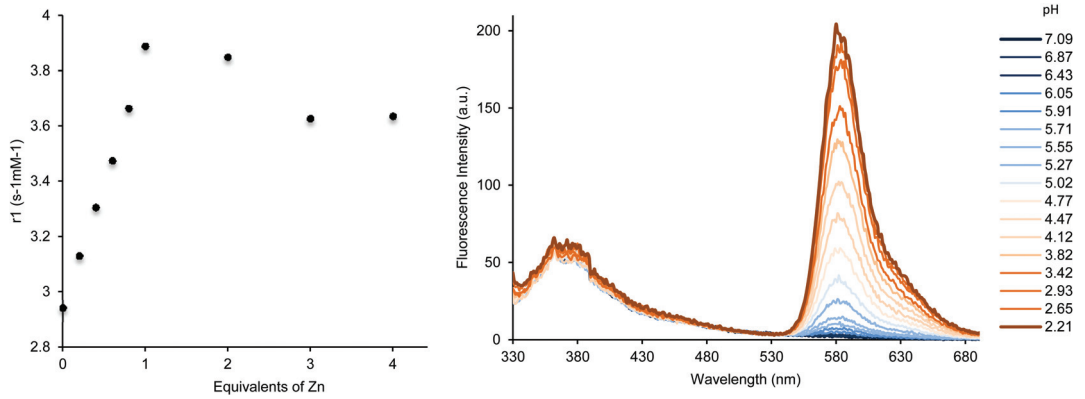

Fig. 4 (Left) Water proton relaxivity of **[GdL^3]** (pH 7.4, 5 mM) in the presence of increasing concentrations (0 to 5 eq.) of Zn^{2+}. (Right) Fluorescence spectra of **[GdL^3]** (100 μM) in 50 : 50 MeOH–water (HEPES buffer, 0.1 M, pH = 7.4) showing an increase in fluorescence at λ = 580 nm upon lowering of pH (λ_{ex} = 260 nm).

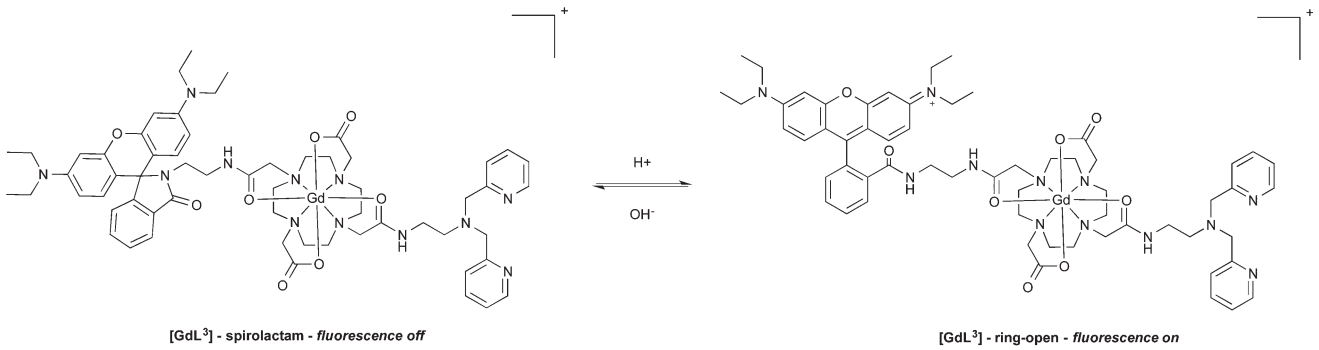

Scheme 4 pH-mediated ring opening of the intramolecular spirolactam of **[GdL^3]**, to give a highly fluorescent species.

be due to the increased steric bulk around the gadolinium centre, as observed in **[GdL^1]**, and secondly with two coordinating amides, the water exchange is significantly reduced. Due to the similarity of **[GdL^3]** to **[GdL^2]** an increase in the observed relaxivity rate was expected upon addition of Zn^{2+} and this was indeed found, with a 31% increase observed. This improved change in the relaxivity rate is most probably attributed to the increased molecular weight of the molecule as a whole, and thus a slowing of the rotational tumbling rate, as well as an increase in the second sphere water ordering.

The UV-vis absorption spectra of the complex were monitored upon addition of Zn^{2+} as well as the biologically relevant cations Cu^{2+}, Mg^{2+} and Ca^{2+}. In comparison to **[GdL^2]**, metal binding processes at the pyridyl groups can no longer be directly observed by UV-vis spectroscopy as the absorption bands of the rhodamine fragment from 220 to 340 nm now dominate the spectra and obscure the characteristic pyridyl absorptions. To show that this probe could function as a dual-modal agent, we studied the fluorescence properties of the rhodamine moiety. Characteristic rhodamine emission was observed at 580 nm when an excitation wavelength of 260 nm was applied (Fig. 4). At pH 7.4, the emission is very weak due to the spirolactam form of the rhodamine moiety being the most prevalent form of the compound, as observed in previous work (Scheme 4). Under acidic conditions, however, the rhodamine fragment ring-opens to regenerate the strong fluorescence at λ = 580 nm as seen in Fig. 4 (right). Although this fluorescence 'switch-on' is not a consequence of zinc binding, we are currently working on using this result to design our next generation of dual-modal MRI/optical zinc sensors. By exploiting the ring-opening mechanism we expect to generate a probe that displays a 'switch-on' in fluorescence in the presence of zinc, whilst maintaining the attractive relaxivity response seen in **[GdL^3]**.

Conclusions

Three first generation MR active zinc selective probes, two of which are dual-modal, based on the cyclen motif have been synthesised. **[GdL^1]**, the dansyl-DO3AMA conjugate, showed slight changes in dansyl fluorescence and a decrease in the relaxation rate from 3.8 to 3.2 mM^{-1} s^{-1} upon zinc addition. These studies lead us to develop **[GdL^2]** in order to probe the effects of the improved zinc-chelating moiety **BPEN**, and also the improved stability of the gadolinium chelate. Although this probe is not dual-modal, we observed an increase in the relaxation rate with increased zinc concentration and this design

led to the design of dual-modal [**GdL^3**]. Using the higher wavelength emitting fluorophore rhodamine, we arrived at the third iteration of the first generation probes. It showed an increase in the relaxation rate from 2.94 to 3.88 mM^{-1} s^{-1} and classical rhodamine fluorescence upon lowering of solution pH. Although [**GdL^3**] proved to be unsuitable as an imaging probe due to its lack of water solubility and lack of change in fluorescence intensity upon zinc addition, we now have a better understanding of what is required of a dual-modal zinc selective probe, and will use these results to design a series of second generation probes that show improved relaxation and NIR fluorescence properties.

Experimental

Materials and conditions

No special precautions were taken to exclude air or moisture during reactions or workups, unless otherwise stated. Products **^{t}Bu-DO3A**,[25] **^{t}Bu-DO2A**,[26] **BPEN**[21] and **5**[8] were prepared *via* literature methods from commercially available starting materials. All other materials were purchased from commercial suppliers and used without further purification.

Instrumentation

^{1}H and ^{13}C{^{1}H} NMR spectra were recorded at ambient temperature on a Bruker 400 MHz spectrometer and internally referenced to the residual solvent peaks of $CDCl_3$ at 7.26 ppm (^{1}H) and 77.16 ppm (^{13}C{^{1}H}) or D_2O at 4.79 ppm (^{1}H). ^{13}C{^{1}H} spectra were fully assigned where possible using 2D correlation spectroscopy. Mass spectrometry analyses were conducted by the Mass Spectrometry Service, Imperial College London. Microanalyses were carried out by Stephen Boyer of the Science Centre, London Metropolitan University.

Fluorescence and UV-Vis measurements

Absorption and fluorescence spectra of all complexes in either aqueous or methanolic solutions depending on solubility were obtained at room temperature on a PerkinElmer Lambda 25 spectrometer and a Cary Varian luminescence spectrometer (using SCAN for Windows), respectively. Samples were held in 10 mm × 4 mm quartz Hellma cuvettes or BRAND UV disposable micro-cuvettes. Excitation and emission slits were set to 10 : 10 nm bandpass, respectively.

Metal ion titrations

100 μM solutions of the gadolinium complexes in either aqueous HEPES buffer or aqueous HEPES–methanol (50 : 50) solutions were prepared. Inorganic salts were dissolved in methanol to afford 0.025, 0.05, 0.1 and 1.25 M solutions. Aliquots of these solutions using the appropriate concentrations were then added to BRAND UV disposable micro-cuvettes and the solvent was allowed to evaporate. The gadolinium complex solution was then added to the metal containing cuvettes (solution stirred for 5 minutes) in order of increasing metal ion concentrations to give solutions of 0 to 5 eq.

pH titration

A 100 μM solution of **GdL^3** in a water–methanol (50 : 50) solution mixture (3 mL) was prepared. The pH of the solution was monitored and adjusted to acidic or basic conditions using aliquots of 1 M HCl or 1 M NaOH, respectively. The pH was allowed to stabilise. Excitation wavelength of 250 nm was used.

Relaxivity measurements

Gadolinium complexes, either in a water solution or a water–methanol 50 : 50 solution mixture, were prepared to give 5 mM concentration solutions. The resulting solutions were placed in 1.7 mm diameter capillaries, which were sealed. The $1/T_1$ measurements were performed on a Bruker Avance 400 spectrometer (400 MHz). The concentration of Gd^{3+} was checked by the chemical shift measurement of HOD induced by magnetic susceptibility (Evans method).[27]

Synthesis of 1. 2-(Aminomethyl)pyridine (0.95 mL, 9.25 mmol) and NEt_3 (1.35 mL, 9.71 mmol) were stirred together in THF (20 mL) and cooled to 0 °C in an ice-water bath. Chloroacetyl chloride (0.77 mL, 9.71 mmol) in THF (10 mL) was added dropwise over an hour. The reaction was monitored by TLC (EtOAc–MeOH = 9/1). After 4 h of stirring at room temperature, the solids were filtered, and the filtrates were concentrated under reduced pressure. The residue was dissolved in EtOAc (40 mL) and extracted with saturated sodium hydrogen carbonate solution (3 × 20 mL). After drying the collective organic layers over magnesium sulphate, the solvent was evaporated under reduced pressure, yielding a light brown oil (1.41 g, 7.62 mmol 82%). ^{1}H NMR ($CDCl_3$): δ = 8.58 (1H, d, $^3J_{HH}$ = 4.76 Hz), 7.89 (1H, s br), 7.69 (1H, dt, $^3J_{HH}$ = 7.69 Hz, $^3J_{HH}$ = 1.76 Hz), 7.25 (2H, m), 4.61 (2H, d, $^3J_{HH}$ = 5.00 Hz), 4.13 (2H, s). ^{13}C NMR ($CDCl_3$): δ = 166.1, 155.5, 149.2, 136.9, 122.6, 122.0, 44.6, 42.6. MS (ES): m/z = 185 $[M + H]^+$.

Synthesis of 2. Dansyl-Cl (1.88 g, 6.97 mmol) dissolved in $CHCl_3$ (30 mL, passed through Al_2O_3) was slowly added to a solution of cyclen (3.00 g, 17.4 mmol) and $CHCl_3$ (60 mL). The resulting clear light green solution was left to stir at room temperature for 48 h. The reaction mixture was concentrated under vacuum and purified *via* column chromatography (DCM–MeOH, 85 : 15) to yield a bright green crystalline solid (1.90 g, 67% yield). ^{1}H NMR ($CDCl_3$), δ: 8.55 (1H, $^3J_{HH}$ = 8.44 Hz), 8.49 (1H, d, $^3J_{HH}$ = 8.72 Hz), 8.22 (1H, dd, $^3J_{HH}$ = 7.30 Hz, $^3J_{HH}$ = 0.86 Hz), 7.59–7.51 (2H, m), 7.19 (1H, d, $^3J_{HH}$ = 7.52 Hz), 3.41 (4H, t, $^3J_{HH}$ = 5.08 Hz), 2.89 (6H, s, CH_3), 2.80–2.75 (8H, m), 2.62 (4H, t, $^3J_{HH}$ = 5.18 Hz). ^{13}C NMR ($CDCl_3$), δ: 151.8, 133.5, 130.7, 130.3, 130.2, 129.7, 128.3, 123.2, 119.4, 115.3, 49.6, 48.6, 47.7, 45.7, 45.4. HR ESMS$^+$ m/z calcd for $C_{20}H_{31}N_5O_2S$ 406.2265 $[M + H]^+$ found 406.2270. Anal. Calcd for $C_{20}H_{31}N_5O_2S$: C, 59.23; H, 7.70; N, 17.27%. Found C, 59.11; H, 7.66; 17.16%.

Synthesis of L^1. Dansyl-cyclen (0.81 g, 1.99 mmol) was stirred together with acetamide (1.12 g, 6.08 mmol) and K_2CO_3 (0.84 g, 6.08 mmol) in MeCN at 60 °C. After 18 h, the solids were filtered off, and the filtrate was reduced under pressure.

The resulting brown oily residue was subjected to column chromatography on alumina (DCM – 1% MeOH), to yield a yellow powder (0.54 g, 32%). ^{1}H NMR ($CDCl_3$), δ: 8.56 (1H, d, $^3J_{HH}$ = 8.44 Hz), 8.49 (2H, dd, $^3J_{HH}$ = 4.92 Hz, $^4J_{HH}$ = 0.84 Hz), 8.35 (1H, d, $^3J_{HH}$ = 8.72 Hz), 8.27 (1H, t, $^3J_{HH}$ = 5.40 Hz), 8.17 (1H, d, $^3J_{HH}$ = 4.72 Hz), 8.02 (2H, t, $^3J_{HH}$ = 5.80 Hz), 7.99 (1H, dt, $^3J_{HH}$ = 7.26 Hz, $^4J_{HH}$ = 1.12 Hz), 7.63 (2H, td, $^3J_{HH}$ = 7.67 Hz, $^4J_{HH}$ = 1.73 Hz), 7.55–7.49 (2H, m), 7.48 (1H, td, $^3J_{HH}$ = 7.69 Hz, $^4J_{HH}$ = 1.73 Hz), 7.26–7.14 (6H, m), 6.89 (1H, dd, $^3J_{HH}$ = 7.18 Hz, $^3J_{HH}$ = 5.14 Hz), 4.52 (4H, d, $^3J_{HH}$ = 5.36 Hz), 4.45 (2H, d, $^3J_{HH}$ = 5.12 Hz), 3.29 (4H, t, $^3J_{HH}$ = 6.02 Hz), 3.19 (2H, s), 3.18 (4H, s), 3.13 (4H, t, $^3J_{HH}$ = 5.94 Hz), 2.91 (6H, s), 2.74 (4H, t, $^3J_{HH}$ = 2.72 Hz), 2.69 (4H, t, $^3J_{HH}$ = 2.60 Hz). ^{13}C NMR ($CDCl_3$), δ: 170.8, 157.0, 156.8, 156.7, 149.4, 149.2, 149.1, 137.3, 136.1, 134.3, 130.6, 130.5, 130.4, 130.3, 128.8, 123.1, 122.8, 122.6, 121.9, 121.8, 121.4, 121.2, 58.5, 57.5, 54.4, 53.2, 45.0, 44.6, 44.5, 44.2, 43.4. MS (ES): m/z = 850 $[M]^+$, 851 $[M + H]^+$, 872 $[M + Na]^+$. Anal. Calcd for $C_{44}H_{55}N_{11}O_5S$: C, 62.17; H, 6.52; N, 18.13%. Found C, 62.30; H, 6.62; N 18.09%.

Synthesis of [GdL^1]. Tri-acetamide-dansyl cyclen (0.25 g, 0.291 mmol) and $Gd(OTf)_3$ (0.16 g, 0.262 mmol) were dissolved in MeCN (30 mL). The solution was heated under reflux for 16 h, and then concentrated. Following flash chromatography with alumina, the resulting yellow solution was concentrated and dissolved in a minimal amount of MeCN, followed by 100 mL of Et_2O then stirring for a week to yield an orange powder (0.32 g, 84%). MS (FAB$^+$): m/z = 1007 $[M]^+$, 1305 $[M + 2CF_3SO_3^-]^{2+}$. Anal. Calcd for $C_{47}H_{55}F_9GdN_{11}O_{14}S_4$: C, 38.81; H, 3.81; N, 10.59%. Found C, 38.70; H, 3.77; N 10.63%.

Synthesis of 4. BPEN (1.45 g, 6.14 mmol) was dissolved in DCM (30 mL), NEt_3 (0.94 mL, 6.75 mmol) was added and the reaction mixture was cooled to 0 °C using an ice bath. Chloroacetyl chloride (0.54 mL, 6.75 mmol) was then added dropwise. The reaction mixture was allowed to rise to room temperature. The solution was stirred for 2 h, then the solvent was removed under reduced pressure. The resultant was re-dissolved in DCM (20 mL) and salts filtered. After removal of DCM the resultant was purified by alumina chromatography with DCM to afford **4** as a pale yellow oil (1.25 g, 64%). ^{1}H NMR (400 MHz, $CDCl_3$) δ (ppm) = 2.93 (t, 2H, $^3J_{HH}$ = 5.6 Hz), 3.47 (m, 2H), 4.04 (s, 2H), 4.07 (s, 4H), 7.34 (m, 2H), 7.55 (d, 2H, $^3J_{HH}$ = 7.6 Hz), 7.80 (td, 2H, $^3J_{HH}$ = 8 Hz, 4 Hz), 8.66 (d, 2H, $^3J_{HH}$ = 5.2 Hz). ^{13}C NMR (100 MHz, $CDCl_3$) δ (ppm) = 37.17, 42.59, 53.30, 58.55, 123.47, 124.62, 138.81, 147.54, 156.11, 166.72. HR ESMS$^+$ m/z calcd for $C_{16}H_{20}N_4OCl$ 319.1326 $[M + H]^+$, found 319.1339.

Synthesis of 5. Tris-*tert*-butyl-DO3A (0.90 g, 1.4 mmol) and K_2CO_3 (0.2 g, 1.6 mmol) were dissolved in MeCN (30 mL) and left to stir for 5 min. **4** (0.50 g, 1.6 mmol) in MeCN (10 mL) was then added dropwise. The reaction mixture was set to reflux for 24 h. The resulting solution was filtered and the filtrate was concentrated under reduced pressure. The crude product was purified by Al_2O_3 chromatography using 1–10% MeOH–DCM, affording **5** as a beige solid (0.68 g, 54%). ^{1}H NMR (400 MHz, $CDCl_3$) δ (ppm) = 1.37 (s, 27H), 2.17–3.41 (m, 28 H), 3.80 (s, 4H), 7.09 (m, 2H), 7.33 (d, 2H, $^3J_{HH}$ = 8 Hz), 7.56 (td, 2H, $^3J_{HH}$ = 7.6 Hz, 1.6 Hz), 8.48 (d, 2H, $^3J_{HH}$ = 4.4 Hz). ^{13}C NMR (100 MHz, $CDCl_3$) δ_C = 28.14, 37.51, 42.67, 44.00, 45.04, 47.09, 49.26, 51.10, 51.43, 52.17, 57.67, 59.91, 81.54, 122.21, 123.62, 149.99, 158.88, 165.86, 169.81, 170.5, 171.73. HR ESMS$^+$ m/z calcd for $C_{42}H_{68}N_8O_7$ 797.5289 $[M]^+$, found 797.5290. Anal. Calcd for $C_{42}H_{68}$ $K_2N_8O_7$: C, 57.64; H, 7.83; N, 12.80%. Found C, 56.90; H, 7.80; N, 12.85%.

Synthesis of L^2. 5 (0.15 g, 0.19 mmol) was dissolved in CH_2Cl_2 (5 mL), and trifluoroacetic acid (5 mL) was added dropwise. The solution was stirred at room temperature, open to air, for 24 h. The solvents were removed *in vacuo* and the residue was redissolved in CH_2Cl_2. This was repeated with diethyl ether and again with CH_2Cl_2 until **L^2** was obtained as a white powder (0.17 g, TFA salts present). ^{1}H NMR (400 MHz, D_2O) δ (ppm) = 2.26 (br, 2H), 2.79–3.83 (br m, 24H), 4.10 (s, 8H), 7.85 (t, 2H, $^3J_{HH}$ = 6.8 Hz), 7.95 (d, 2H, $^3J_{HH}$ = 8 Hz), 8.40 (t, 2H, $^3J_{HH}$ = 7.6 Hz), 8.56 (d, 2H, $^3J_{HH}$ = 5.6 Hz). ^{13}C NMR (100 MHz, D_2O) δ_C = 36.66, 49.25, 51.34, 53.98, 55.29, 117.70, 126.31, 127.35, 141.83, 147.83, 152.40, 162.98, 174.05, 174.60. HR ESMS$^+$ m/z calcd for $C_{30}H_{45}N_8O_7$ 629.3411$[M + H]^+$, found 629.3428.

Synthesis of [GdL^2]. **L^2** (0.10 g, 0.16 mmol) and $GdCl_3{\cdot}6H_2O$ (0.059 g, 0.16 mmol) were dissolved in water (4 mL), and the pH was adjusted to 5.5 using 2 M NaOH solution. The mixture was stirred at room temperature for 24 h. The pH was increased to 10 by the addition of 2 M NaOH to precipitate the uncomplexed Gd^{3+}, the pH was brought to 7.4 and water was removed. The residue was purified by Sephadex G10 desalting resin to yield **[GdL^2]** as a white powder (0.0091 g, 7%). HR ESMS$^+$ m/z calcd for $C_{30}H_{42}GdN_8O_7$ 784.2418 $[M + H]^+$, found 784.2446. r_1 (H_2O, 298 K, 400 MHz) = 4.55 $mmol^{-1}$ s^{-1}; λ_{abs} = 262 nm.

Synthesis of 6. Bis-*tert*-butyl-DO2A (1.50 g, 3.8 mmol) and K_2CO_3 (0.52 g, 3.8 mmol) were dissolved in MeCN (130 mL) and left to stir for 5 min. **5** (2.11 g, 3.8 mmol) was then added. The reaction mixture was set to reflux for 24 h. The resulting solution was filtered and the filtrate was concentrated under reduced pressure. The crude product was purified by Al_2O_3 chromatography using 1–2% MeOH–DCM, affording **6** as a pale pink solid (1.59 g, 46%). ^{1}H NMR (400 MHz, $CDCl_3$) δ (ppm) = 1.17 (t, 12H, $^3J_{HH}$ = 7.2 Hz), 1.47 (s, 18H), 2.40–3.10 (series of multiplets, 24H), 3.22 (m, 2H), 3.32 (q, 8H $^3J_{HH}$ = 7.2 Hz), 6.30 (dd, 2H, $^4J_{HH}$ = 2.6 Hz, $^3J_{HH}$ = 8.8 Hz), 6.39 (d, 2H, $^4J_{HH}$ = 2.6 Hz), 6.50 (d, 2H, $^3J_{HH}$ = 8.8 Hz), 7.06 (m, 1H), 7.43 (m, 2H), 7.92 (m, 1H), 8.08 (br s, 1H). ^{13}C NMR (100 MHz, $CDCl_3$) δ_C = 12.65, 28.22, 37.70, 39.86, 44.33, 48.78, 52.44, 53.42, 55.86, 56.85, 57.21, 64.90, 80.91, 97.82, 105.32, 108.20, 122.85, 123.74, 127.95, 128.70, 130.61, 132.44, 148.80, 153.14, 153.98, 168.56, 170.89, 171.98. HR ESMS$^+$ m/z calcd for $C_{52}H_{77}N_8O_7$ 925.5915 $[M]^+$, found 925.5920. Anal. Calcd for $C_{52}H_{76}N_8O_7$: C, 67.50; H, 8.28; N, 12.11%. Found C, 67.39; H, 8.17; N, 12.02%.

Synthesis of 7. 6 (1.20 g, 1.3 mmol) and K_2CO_3 (0.20 g, 1.6 mmol) were dissolved in MeCN (40 mL) and left to stir for 5 min. **4** (0.50 g, 1.5 mmol) in MeCN (10 mL) was then added dropwise. The reaction mixture was set to reflux for 24 h. The

resulting solution was filtered and the filtrate was concentrated under reduced pressure. The crude product was purified by Al_2O_3 chromatography using 1–10% MeOH–DCM, affording **7** as a beige solid (0.68 g, 34%). ^{1}H NMR (400 MHz, $CDCl_3$) δ (ppm) = 1.14 (t, 12H, $^3J_{HH}$ = 6.8 Hz), 1.35 (s, 18H), 2.47–3.56 (series of multiplets, 28H), 3.32 (q, 8H, $^3J_{HH}$ = 6.8 Hz), 3.82 (s, 4H), 6.35 (br m, 6H), 7.04 (m, 1H), 7.12 (m, 2H), 7.40 (m, 2H), 7.64 (m, 4H), 7.80 (m, 1H), 8.46 (d, 2H, $^3J_{HH}$ = 4.8 Hz), 9.81 (t, 1H, $^3J_{HH}$ = 5.3 Hz), 10.57 (t, 1H, $^3J_{HH}$ = 5.5 Hz). ^{13}C NMR (100 MHz, $CDCl_3$) δ_C = 12.63, 27.97, 38.03, 38.95, 39.85, 44.29, 48.78, 50.27, 53.25, 56.83, 57.04, 59.96, 65.17, 86.25, 97.74, 122.04, 122.96, 123.34, 123.71, 127.88, 130.00, 132.64, 136.69, 148.80, 154.08, 159.20, 169.07, 173.52, 174.54. HR ESMS$^+$ *m*/*z* calcd for $C_{68}H_{94}N_{12}NaO_8$ 1229.7215 $[M + Na]^+$. Found 1229.7219.

Synthesis of L^3. **5** (0.44 g, 0.36 mmol) was dissolved in CH_2Cl_2 (10 mL), and trifluoroacetic acid (10 mL) was added dropwise. The solution was stirred at room temperature, open to air, for 24 h. The solvents were removed *in vacuo* and the residue was redissolved in CH_2Cl_2. This was repeated with diethyl ether and again with CH_2Cl_2 until **L^3** was obtained as a bright pink powder (0.13 g, TFA salts present). ^{1}H NMR (400 MHz, D_2O) δ (ppm) = 1.03 (t, 12H, $^3J_{HH}$ = 7.2 Hz), 2.69–3.46 (series of multiplets, 32H), 3.55 (q, 8H, $^3J_{HH}$ = 7.2 Hz), 4.12 (s, 4H), 6.98 (d, 2H, $^3J_{HH}$ = 8.8 Hz), 7.09 (dd, 1H, $^3J_{HH}$ = 6 Hz, $^4J_{HH}$ = 2 Hz), 7.12 (dd, 2H, $^3J_{HH}$ = 8.4 Hz, $^4J_{HH}$ = 2 Hz), 7.51 (d, 2H, $^3J_{HH}$ = 2 Hz), 7.56 (m, 2H), 7.79 (t, 2H, $^3J_{HH}$ = 6.8 Hz), 7.87 (m, 1H), 7.94 (d, 2H, $^3J_{HH}$ = 8 Hz). ^{13}C NMR (100 MHz, D_2O) δ_C = 9.63, 14.08, 53.82, 54.98, 65.98, 110.00, 111.93, 112.19, 114.83, 117.73, 118.26, 120.33, 126.30, 127.25, 130.80, 138.46, 141.74, 147.25, 152.04, 152.45, 161.22, 162.57, 162.93. HR ESMS$^+$ *m*/*z* calcd for $C_{60}H_{78}N_{12}O_8$ 1095.6144 $[M]^+$. Found 1095.6125.

Synthesis of [GdL^3]. **L^3** (0.30 g, 0.27 mmol) and $GdCl_3{\cdot}6H_2O$ (0.10 g, 0.27 mmol) were dissolved in water (12 mL), and the pH was adjusted to 5.5 using 2 M NaOH solution. The mixture was stirred at room temperature for 24 h. The precipitate formed was filtered and washed with water. It was then dissolved in a 50 : 50 MeOH–water mixture and the pH of the solution was increased to 10 by addition of 2 M NaOH to precipitate uncomplexed $Gd(OH)_3$. After the pH was brought to 5.5, DOWEX Mac-3 weak acid-cation exchange resin beads were added and the solution was stirred for 10 min. After removal of the bead and solvent, **[GdL^3]** was obtained as a pale brown powder (0.092 g, 29%). HR ESMS$^+$ *m*/*z* calcd for $C_{60}H_{76}GdN_{12}O_8$ 1250.5150 $[M]^+$. Found 1250.5151.

Notes and references

1 E. L. Que, D. W. Domaille and C. J. Chang, *Chem. Rev.*, 2008, **108**, 1517.
2 G. Parkin, *Chem. Rev.*, 2004, **104**, 699.
3 W. Moret and Y. Li, *Chem. Rev.*, 2009, **109**, 4682.
4 L. Frullano and T. J. Meade, *J. Biol. Inorg. Chem.*, 2007, **12**, 939.
5 S. Aime, S. G. Criche, E. Gianolino, G. B. Giovenzana, L. Tei and E. Terreno, *Coord. Chem. Rev.*, 2006, **250**, 1562.
6 X. A. Zhang, K. S. Lovejoy, A. Jasanoff and S. J. Lippard, *Proc. Natl. Acad. Sci. U. S. A.*, 2007, **104**, 10780; J. L. Major and T. J. Meade, *Acc. Chem. Res.*, 2009, **42**, 893; Y. You, E. Tomat, K. Hwang, T. Atanasijevic, W. Nam, A. P. Jasanoff and S. J. Lippard, *Chem. Commun.*, 2010, 4139; D. Dong, X. Jing, X. Zhang, X. Hu, Y. Wu and C. Duan, *Tetrahedron*, 2012, **68**, 306.
7 Z. Xu, J. Yoon and D. R. Spring, *Chem. Soc. Rev.*, 2010, **39**, 1996; E. Tomat and S. J. Lippard, *Curr. Opin. Chem. Biol.*, 2010, **14**, 225; L. M. De León-Rodríguez, A. J. M. Lubag Jr. and A. D. Sherry, *Inorg. Chim. Acta*, 2012, **393**, 12.
8 C. Rivas, G. J. Stasiuk, J. Gallo, F. Minuzzi, G. A. Rutter and N. J. Long, *Inorg. Chem.*, 2013, **52**, 14284; L. E. Jennings and N. J. Long, *Chem. Commun.*, 2009, 3511; G. J. Stasiuk and N. J. Long, *Chem. Commun.*, 2013, **49**, 2732; K. Guo, M. Y. Berezin, J. Zheng, W. Akers, F. Lin, B. Teng, O. Vasalatiy, A. Gandjbakhche, G. L. Griffiths and S. Achilefu, *Chem. Commun.*, 2010, **46**, 3705.
9 J. Luo, W.-S. Li, P. Xu, L.-Y. Zhang and Z.-N. Chen, *Inorg. Chem.*, 2012, **51**, 9508.
10 É. Tóth, L. Helm and A. E. Merbach, *Top. Curr. Chem.*, 2002, **221**, 61.
11 Z. Xu, J. Yoon and D. R. Spring, *Chem. Soc. Rev.*, 2010, **39**, 1996.
12 K. Hanaoka, K. Kikuchi, Y. Urano and T. Nagano, *J. Chem. Soc., Perkin Trans. 2*, 2001, 1840.
13 A. C. Esqueda, J. A. López, G. Andreu-de-Riquer, J. C. Alvarado-Monzón, J. Ratnaker, A. J. M. Lubag, A. D. Sherry and L. M. De León-Rodríguez, *J. Am. Chem. Soc.*, 2009, **131**, 11387.
14 M. S. T. Gonçalves, *Chem. Rev.*, 2009, **109**, 190.
15 K. Koike, T. Watanabe, S. Aoki, E. Kimura and M. Shiro, *J. Am. Chem. Soc.*, 1996, **118**, 12696; S. Aoki, H. Kawatani, T. Goto, E. Kimura and M. Shiro, *J. Am. Chem. Soc.*, 2001, **123**, 1123; M. P. Lowe and D. Parker, *Inorg. Chim. Acta*, 2001, **317**(1–2), 163.
16 A. J. Parola, J. C. Lima, F. Pina, J. Pina, J. Seixas de Melo, C. Soriano, E. García-España, R. Aucejo and J. Alarcón, *Inorg. Chim. Acta*, 2007, **360**, 1200.
17 P. Caravan, *Chem. Soc. Rev.*, 2006, **35**, 512.
18 S. Sung, H. Holmes, L. Wainwright, A. Toscani, G. J. Stasiuk, A. J. P. White, J. D. Bell and J. D. E. T. Wilton-Ely, *Inorg. Chem.*, 2014, **53**, 1989.
19 A. Mishra, J. Pfeuffer, R. Mishra, J. Engelmann, A. K. Mishra, K. Ugurbil and N. K. Logothetis, *Bioconjugate Chem.*, 2006, **17**, 773.
20 D. Buccella, J. A. Horowitz and S. J. Lippard, *J. Am. Chem. Soc.*, 2011, **133**, 4101.
21 K. Hanaoka, K. Kikuchi, H. Kojima, Y. Urano and T. Nagano, *J. Am. Chem. Soc.*, 2004, **126**, 12470.
22 A. Barge, G. Cavrotto, E. Gianolio and F. Fedeli, *Contrast Media Mol. Imaging*, 2006, **1**, 184.

23 S. J. A. Pope and R. H. Laye, *Dalton Trans.*, 2006, 3108.
24 M. Beija, C. A. M. Afonso and J. M. G. Martinho, *Chem. Soc. Rev.*, 2009, **38**, 2410.
25 B. Jagadish, G. L. Brickert-Albrecht, G. S. Nichol, E. A. Mash and N. Raghunand, *Tetrahedron Lett.*, 2011, **52**(17), 2058.
26 L. M. De León-Rodríguez, Z. Kovacs, A. C. Esqueda-Oliva and A. D. Miranda-Olvera, *Tetrahedron Lett.*, 2006, **47**, 6937; T. Hirayama, M. Taki, A. Kodan, H. Kato and Y. Yamamoto, *Chem. Commun.*, 2009, 3196.
27 D. M. Corsi, C. Platas-Iglesias, H. van Bekum and J. A. Peters, *Magn. Reson. Chem.*, 2001, **39**, 723.